



Sun Guangzheng (Orcid ID: 0000-0002-8353-4109)

Amtmann Anna (Orcid ID: 0000-0001-8533-121X)

Pieterse Corné (Orcid ID: 0000-0002-5473-4646)

Running Title: Arp2/3-mediated pathogen defense signaling.

Highlights:

1. *ShARPC3* showed positive regulation of plant immunity against *Oidium neolycopersici*.
2. Silencing of *ShARPC3* in tomato resulted in enhanced susceptibility.
3. Over-expression of *ShARPC3* in *Arabidopsis thaliana* showed enhanced resistance.
4. Heterologous expression of *ShARPC3* in *Saccharomyces cerevisiae arc18* mutant resulted in complementation of stress-induced phenotypes.

Corresponding authors: Brad Day (MSU) and Qing Ma (NWAUFU)

Department of Plant, Soil and Microbial Sciences

1066 Bogue Street, A286

East Lansing, MI 48824 USA

Telephone: +1 (517) 353-7991

Email: bday@msu.edu

State Key Laboratory of Crop Stress Biology for Arid Areas

College of Plant Protection

Northwest A&F University

This article has been accepted for publication and undergone full peer review but has not been through the copyediting, typesetting, pagination and proofreading process which may lead to differences between this version and the Version of Record. Please cite this article as doi: 10.1111/pce.13569

Yangling, Shaanxi 712100, China

Email: maqing@nwsuaf.edu.cn

**The tomato Arp2/3 complex is required for resistance to the powdery mildew fungus
*Oidium neolycopersici***

Guangzheng Sun^{1†}, Chanjing Feng^{1†}, Jia Guo¹, Ancheng Zhang¹, Yuanliu Xu¹, Yang Wang¹, Brad Day^{2,3,*} and Qing Ma^{1*}

¹ State Key Laboratory of Crop Stress Biology for Arid Areas, College of Plant Protection, Northwest A&F University, Yangling, Shaanxi 712100, China

² Department of Plant, Soil and Microbial Sciences, Michigan State University, East Lansing, MI 48824, USA,

³ Plant Resilience Institute, Michigan State University, East Lansing, MI 48824, USA

*For correspondence (e-mails bday@msu.edu; maqing@nwsuaf.edu.cn).

† These authors have contributed equally to this work.

Abstract

The actin related protein 2/3 complex (Arp2/3 complex), a key regulator of actin cytoskeletal dynamics, has been linked to multiple cellular processes, including those associated with response to stress. Herein, the *Solanum habrochaites* *ARPC3* gene, encoding a subunit protein of the Arp2/3 complex, was identified and characterized. *ShARPC3* encodes a 174-amino-acid protein possessing a conserved P21-Arc domain. Silencing of *ShARPC3* resulted in enhanced susceptibility to the powdery mildew pathogen *Oidium neolycopersici* (*On-Lz*), demonstrating a role for *ShARPC3* in defense signaling. Interestingly, a loss of *ShARPC3* coincided with enhanced susceptibility to *On-Lz*, a process that we hypothesize is the result of a block in the activity of SA-mediated defense signaling. Conversely, over-expression of *ShARPC3* in *Arabidopsis thaliana*, followed by inoculation with *On-Lz*, showed enhanced resistance, including the rapid induction of hypersensitive cell death and the generation of reactive oxygen. Heterologous expression of *ShARPC3* in the *arc18* mutant of *Saccharomyces cerevisiae* (i.e., $\Delta arc18$) resulted in complementation of stress-induced phenotypes, including high temperature tolerance. Taken together, these data support a role for *ShARPC3* in tomato through positive regulation of plant immunity in response to *O. neolycopersici* pathogenesis.

Keywords: Powdery mildew, ARPC3, resistance, *Solanum habrochaites*, Arp2/3 complex, actin cytoskeleton.

Introduction

Tomato powdery mildew, *Oidium neolycopersici*, is an obligate biotrophic fungus which can parasitize more than 60 plant species in 13 families, including members of the *Solanaceae* (Jones *et al.*, 2001). Upon infection of a susceptible host, *O. neolycopersici* causes powdery white lesions on the adaxial tomato leaf surface, abaxial surfaces, petioles, and the calyx; only the fruit remains uninfected. Pathogen infection typically affects leaves of the host plant, causing up to 50% yield losses (fruit) as a result of loss of vigor (Roberts *et al.*, 2002), and has caused devastating epidemics from Europe to North and South America, as well as in Asia (Lebeda *et al.*, 2014). At present, chemical control remains the primary method to manage tomato powdery mildew in greenhouse production; however, chemical fungicide application introduces numerous inherent risks, including the development of pathogen resistance and the accumulation of toxic residues in fruit, both of which pose potential risks to the environment (Nakajima & Akutsu, 2014).

Plants defense signaling in response to bacterial and fungal pathogen infection is mediated by at least two primary nodes of the host innate immune system (Jones & Dangl, 2006). The first, pathogen-associated molecular pattern (PAMP)-triggered immunity (PTI), is often sufficient to protect plants against most pathogens, and is often described as a mechanism of nonhost (basal) resistance (Marcel *et al.*, 2008). In response to PTI, pathogens evolved mechanisms counter host defenses, a process that functions via the delivery of virulence molecules which target a variety of host functions, including immune signaling. To counter this pathogen virulence function, plants evolved to recognize and respond to effector delivery, a process known as effector-triggered immunity (ETI). In short, ETI results in the activation of robust immune signaling, often characterized by localized cell death (i.e., the hypersensitive response; HR) and the subsequent halt of pathogen growth and proliferation (Chisholm *et al.*, 2006).

To date, most of the cloned resistance (*R*) genes encode proteins with an N-terminal nucleotide-binding site (NBS) and C-terminal leucine-rich repeats (LRRs) (Takken *et al.*, 2006). In wild tomato species, several *R* genes have been identified, including six monogenic genes comprising five dominant (*OI-1*, *OI-3*, *OI-4*, *OI-5*, *OI-6*) one recessive (*oi-2*) loci, and three polygenic resistance quantitative trait loci (QTLs) (Bai *et al.*, 2003, 2005). In brief,

OI-4-mediated resistance relies on the salicylic acid (SA) pathway, while *OI-1* and *OI-qtls* require ethylene (ET) to promote delayed cell death during powdery mildew resistance, and jasmonic acid (JA) deficiency can compromise resistance mediated by *oi-2* (Lindhout *et al.*, 1994a, b; Ciccarese *et al.*, 2000; Bai *et al.*, 2003, 2005; Pei *et al.*, 2011). In all instances, resistance to *O. neolyopersici* is associated with the induction of the HR, with a high frequency of necrosis in epidermal cells accompanying H₂O₂ accumulation induced by the fungal haustoria (Bai *et al.*, 2005). Interestingly, when cells undergo the HR, uninfected neighboring cells show an accumulation of focal actin microfilaments (AFs) (Kobayashi *et al.*, 1994).

The eukaryotic cytoskeleton forms a contiguous network within all cells and includes microtubules (MT) and AF systems, both of which are associated with the function of numerous cellular processes (Kim *et al.*, 2005; Sparkes *et al.*, 2009; Yokota *et al.*, 2009; Day *et al.*, 2011; Li & Day, 2019). In short, MTs are hypothesized to play a role in maintaining cell polarity, whereas AFs ensure the targeted delivery of vesicles that carry plasma membrane and cell wall components to the site of growth (Mathur & Hülskamp, 2002). Additionally, AFs support the formation of penetration barriers by recruiting defense-related products to the subcellular site of fungal attack (Opalski *et al.*, 2005). As a putative mechanism underpinning actin-associated defense signaling, work by Henty-Ridilla *et al.* (2013) and Shimono *et al.* (2016a) noted that early transient accumulation of actin (i.e., increased density and decreased filament bundling) is associated with the activation of PTI. Additional evidence points to the requirement for a suite actin-binding proteins (ABPs), including the actin related protein 2 and 3 (Arp2/3) complex, profilin, and actin depolymerizing factors (ADF) (reviewed in Porter & Day, 2015).

A key step in AF organization is actin nucleation, the key rate-limiting step necessary to ensure proper filaments formation (Campellone & Welch, 2010); this process is regulated by the Arp2/3 complex (Chesarone & Goode, 2009). The Arp2/3 complex contains seven subunits, including two actin-related proteins (ARP2 and ARP3) and five unrelated subunits (Machesky *et al.*, 1994, 1999). In eukaryotes, this complex facilitates branched actin network nucleation associated with regions of the plasma membrane (Pollard & Borisy, 2003; Weaver *et al.*, 2003), and is involved in actin polymerization-mediated motility of organelles (Welch *et*

al., 1994; Machesky & Gould, 1999). Interestingly, Mathur *et al.* (2003) found that expansion growth in *Arabidopsis* requires ARP2/3 activity, and its loss results in inefficient fine F-actin formation, leading to enhanced F-actin aggregation and bundling.

At a fundamental level, the Arp2/3 complex polymerizes new AFs in response to suite of signals, including those associated with growth, development, and response to external stimuli (Pollard *et al.*, 2000; Pantaloni *et al.*, 2001; Takenawa & Miki, 2001). Interestingly, the seven subunits serve distinct roles in numerous developmental processes. For example, Arp2 is essential for membrane association (Kotchoni *et al.*, 2009), while Arp3 is primarily associated with sites of actin nucleation (Maisch *et al.*, 2009). Further research also demonstrated that deletion of *ARPC1* or *ARPC2* resulted in lethality and severe reductions in viability in *Saccharomyces cerevisiae*. In plants, Mathur *et al.* (2003a, b) observed that loss-of-function mutants in *Arabidopsis* ARP3 or ARPC5 leads to shorter and sometimes sinuous root hairs. As a function of plant immunity, recent work by Qi *et al.* (2017) demonstrated that *TaARPC3* is a key subunit of the Arp2/3 complex that is required for wheat resistance against *Puccinia striiformis* f. sp. *tritici*.

In the current study, we found that expression of *ShARPC3* was significantly up-regulated during an incompatible host-pathogen interaction, suggestive of a role for *ShARPC3* in plant defense signaling and immunity. This is significant, as a defined role for Arp2/3 signaling during plant pathogenesis by fungal pathogens has not been described. Using the model plant tomato and infection by the powdery mildew pathogen *O. neolycopersici*, we describe a function for *ShARPC3* during infection and defense signaling in tomato. In total, the current study contributes to a broader understanding of the role of the Arp2/3 complex in pathogen defense signaling, and moreover, sheds light on the regulation of this complex in growth, development, and response to stress.

Results

Identification and sequence analysis of tomato ARPC3

A tomato 525-bp homolog of actin related protein was isolated from tomato LA1777 by

homology-based cloning and the obtained cDNA was designated as *ShARPC3*. Blast analysis of *ShARPC3* nucleotide sequence in the Tomato Genome CDS (ITAG release 3.20) database revealed that one copy was present, localized on chromosome 7. The predicted ORF of *ShARPC3* encodes a protein of 174 amino acid with a predicted molecular weight of 21 kDa. As shown in Figure 1A, phylogenetic analysis of *ShARPC3* with other tomato ARP2/3 complex members and other species ARP2/3 complex members revealed that *ShARPC3* clusters with *AtARPC3* (AT1G60430) and *NtARPC3* (XM_009610279), all of which are members of actin related proteins in dicotyledons. Amino acid sequences alignment of *ShARPC3* with *AtARPC3*, *NsARPC3* (XP_009791878), *NtARPC3* (XP_009608574), *BnARPC3* (XP_022548276), *SbARPC3* (XP_002451839), *VrARPC3* (XP_014510301), and *OsARPC3* (XP_015626361) predicts that *ShARPC3* encodes a protein with unique conserved domains also found in the ARP2/3 complex-containing subunit ARPC3 (Fig. 1B). *In silico*-based sequence analysis revealed that *ShARPC3* has high sequence similarity to *AtARPC3* and *NtARPC3*, with identities of 86% and 93%, respectively. SMART and RCSB PDB analyses revealed that *ShARPC3* possesses a conserved Pfam:P21-Arc domain (amino acids 1-173), one glycyl lysine isopeptide (Lys-Gly) (interchain with G-Cter in SUMO2)-cross-link site (amino acid 14), one phosphotyrosine-modified residue (amino acid 47), and two N6-acetyllysine-modified residues (amino acids 56 and 61). These data reveal that *ShARPC3* is closely related to *AtARPC3* and *NtARPC3*.

Using an *in silico*-based approach (e.g., STRING database analysis), we generated a predicted protein network map (Fig. 1C; high confidence score = 0.982), which revealed interactions between tomato ARPC3 and numerous additional tomato proteins. As shown, tomato ARPC3 is predicted to interact with actin-related protein 2/3 complex subunit 1A (ARPC1A), ARP2/3 complex subunit 1B (ARPC1B), ARP2/3 complex subunit 2 (ARPC2), ARP2/3 complex subunit 4 (ARPC4), ARP2/3 complex subunit 5 (ARPC5), ARP2/3 complex subunit 5-like protein (ARPC5L), ARP2 (ACTR2), ARP3 (ACTR3), ARP3B (ACTR3B), and Neural Wiskott-Aldrich syndrome protein (WASL). In total, the interaction map contains a total 11 nodes with 54 edges, and further analysis indicates that all of these tomato proteins are involved in actin cytoskeletal organization, mitosis, and cytokinesis. Based on this, we hypothesize that *ShARPC3* functions through dynamic interactions with other ARP2/3

complex subunits to regulate cellular morphology, as well as abiotic and biotic signaling responses.

ShARPC3 is localized in the cytoplasm and plasma membrane in tomato protoplast

Based on the analysis above, we hypothesized that *ShARPC3* is localized within multiple subcellular environments, including plasma membrane, extracellular spaces, cytoplasm, mitochondria, endoplasmic reticulum, peroxisomes, Golgi, and chloroplast (Supplementary Table S4). To further determine the precise subcellular localization of *ShARPC3*, the *ShARPC3* ORF was fused to GFP and placed under the control of the constitutive *Cauliflower mosaic virus* 35S promoter, and transiently expressed in tomato protoplasts. As shown in Figure 2, pCaMV35S:*GFP* (negative control) revealed a diffuse, non-specific cellular address, while cells expressing GFP-tagged *ShARPC3* was localized predominantly in the cytoplasm and nucleus.

ShARPC3 does not induce the hypersensitive cell death response nor suppress BAX-induced necrosis

To further define *ShARPC3* function, we next employed a PVX-based high-throughput transient plant over-expression system under the regulation of the 35S promoter, using *Nicotiana benthamiana*, to evaluate ARPC3 function and activity during cell death elicitation. As shown in Supplementary Fig. S1, infiltration of *N. benthamiana* leaves with *Agrobacterium* expressing pGR106:*GFP* (site 'a', CK), pGR106:*ShARPC3* (site 'b'), or buffer alone (site 'c') did not result in the induction of cell-death symptoms. These data indicate that ARPC3 does not possess cell-death-inducing activity. To determine if the over-expression of ARPC3 can positively, or negatively, influence BAX-induced cell death, *N. benthamiana* leaves were infiltrated with *Agrobacterium* cells harboring *ShARPC3* gene 24 h prior to infiltration with the pGR106:*BAX*-harboring cells produced cell-death symptoms (Fig. S1, site 'e'). As expected, cell death was observed in *N. benthamiana* leaves infiltrated with *Agrobacterium* cells expressing pGR106:*GFP*:*BAX* (Fig. S1, site 'd'). As shown, the BAX-induced cell death

response, in the presence of ARPC3, was no different than over-expression of BAX alone (Fig. S1, site 'f').

ShARPC3 is differentially induced by On-Lz infection

To determine the expression profile of *ShARPC3*, the mRNA accumulation of *ShARPC3* was monitored during the interaction between tomato and *On-Lz* using qRT-PCR. LA1777 plants showed resistance against *On-Lz*, whereas obvious powdery mildew disease lesions appeared in MM plants (Supplementary Fig. S2A). The disease indexes of MM plants were significantly higher, with lesion indices reaching 18.5 and 26.4 at 7 and 14 dpi, respectively (Supplementary Fig. S2B). As shown in Figure 3, during an incompatible interaction, *ShARPC3* transcripts were significantly up-regulated at 12–24 hpi, and mRNA accumulation peaked at 18 hpi, 16 times ($P < 0.05$) than that in control (uninoculated) plants. Additionally, *ShARPC3* transcript levels were much higher during an incompatible interaction than during a compatible interaction at all time points evaluated, except at 96 hpi. Based on this, we hypothesize that *ShARPC3* is associated with resistance of tomato against *On-Lz* infection.

Silencing of ShARPC3 results in host susceptibility to On-Lz

To determine the role of *ShARPC3* during tomato infection by *On-Lz*, we used a tobacco rattle virus-induced gene silencing (TRV-VIGS)-based approach to silence *ShARPC3* expression in LA1777. As shown in Figure 4, TRV2 (CK), TRV2:*ShPDS* (phytoene desaturase), and TRV2:*ShARPC3* plasmids, were inoculated onto tomato leaves for silencing. As expected, plants inoculated with TRV2:*ShPDS* showed a photobleaching phenotype at ~30 days post-inoculation (Fig. 4A), indicating the induction of TRV-VIGS-mediated silencing. At this point (i.e., 30 dpi), all plants were inoculated with *On-Lz* and infection phenotypes were recorded. Compared to control plants, plants carrying TRV2:*ShARPC3* showed obvious powdery mildew disease spot lesions (Fig. 4A), and the disease indexes of *ShARPC3*-silenced plants were significantly higher, with lesion indices reaching 10.7 and 21.1 at 7 and 14 dpi, respectively (Fig. 4B). In parallel, samples were collected to assess the

efficiency of gene silencing using qRT-PCR analysis. The expression of *ShARPC3* was reduced by 60-85% at 0-72 hpi compared with control-inoculated leaves (Supplementary Fig. S3); *ShARPC3*-silenced efficiency peaked at 24 hpi. Based on these data, we conclude that *ShARPC3* is required for resistance to *On-Lz*.

Silencing of ShARPC3 results in reduced defense responses following On-Lz inoculation

To further investigate how *ShARPC3* participates in tomato resistance to *On-Lz*, we measured the accumulation of H_2O_2 and the development of the HR at 6, 18, 24, 48, and 72 hpi via a microscopic examination of the infection process (Fig. 5). As shown, a histological examination of *On-Lz* growth was performed in both control and *ShARPC3*-silenced plants by analyzing the HR production rate (Fig. 5A, C). We found that HR production in the *ShARPC3*-silenced plants was much less compared with the control plants at 48 and 72 hpi ($P < 0.05$). There were no obvious differences between TRV2-treated and *ShARPC3*-silenced plants in HR production at 18 and 24 hpi. As the infection progressed, we also observed a significant decrease in the amount of H_2O_2 accumulated in *ShARPC3*-silenced plants (leaves) at 72 hpi ($P < 0.05$); H_2O_2 was 0.45 times that in TRV2-treated leaves (CK) (Fig. 5B, D). Additionally, with the increase of haustoria formation, more invasive growth in *ShARPC3*-silenced plants was observed than in control plants. Taken together, these results indicate that a reduction in *ShARPC3* expression compromises resistance signaling in response to *On-Lz* infection.

Effects of ShARPC3 silencing on phytohormone accumulation and PR transcript levels

To confirm the relevance of *ShARPC3* expression as a function of the activity of SA signaling pathway, we measured SA level in *ShARPC3*-silenced plants at 0–24 hpi with *On-Lz*. As shown in Figure 6A, in control plants (CK), SA content reached its highest level of $1818.0 \mu\text{g}\cdot\text{g}^{-1}$ at 12 hpi, > 2.5 times that in *ShARPC3*-silenced plants. Additionally, SA levels were significantly lower in *ShARPC3*-silenced plants than in the control plants at all time points, and higher than that at 0 hpi. We further studied pathogenesis-related (PR) *PR1b1* (*PR1*),

Glucanase A (PR2), Glucanase B (PR2-like), Chitinase 3 (PR3), and Chitinase 9 (PR3-like) gene expression after inoculation with *On-Lz*. In *ShARPC3*-silenced plants at 24 hpi, the expressions of *PR1*, *PR2* and *PR3* genes (SA pathway-specific gene expression markers) were significantly reduced (Fig. 6B). Taken together, we posit that *ShARPC3* is required for the positive regulation of host defenses, mediated in part by SA signaling.

Overexpression of ShARPC3 functionally complements the arpc3 mutation

To test whether *ShARPC3*-based resistance occurs in Arabidopsis, we evaluated a homozygous *arpc3* mutant, an *arpc3* complementation line, and WT Col-0 plants over-expressing *ShARPC3* under the regulation of the 35S promoter and challenged them with *On-Lz*. As expected, macroscopic inspection revealed that *arpc3* plants were susceptible to *On-Lz* (Fig. 7B). However, *arpc3* complementation plants, like the control plants (i.e., WT Col-0), showed only slight disease symptoms following infection. Conversely, WT Col-0 plants carrying 35S:pCAMBIA3301-*ShARPC3* showed no obvious symptoms, possibly due to the additive effect of native + transgene over-expression of *ShARPC3*. Microscopic examination revealed that resistance in *arpc3* plants carrying 35S:pCAMBIA3301-*ShARPC3* and WT Col-0 plants carrying 35S:pCAMBIA3301-*ShARPC3* was incomplete and characterized by reduced conidiophore and haustorium formation (Fig. 7C, D, E). Compared with control plants (i.e., WT Col-0), conidiophore production was significantly higher in *arpc3* mutant plants ($P < 0.05$). Additionally, the growth ability of the complemented *arpc3* plants containing 35S:pCAMBIA3301-*ShARPC3* was stronger than that in the *arpc3* mutant, yet weaker than that in WT Col-0 plants (Fig. 7A).

Resistance mechanisms revealed in histological and biochemical studies

To assess the impact of *ARPC3* on the response of Arabidopsis to *On-Lz*, we next investigated the host response via a microscopic examination of the infection process. To do this, we measured the development of the HR (Fig. 8A, C) and the accumulation of H_2O_2 (Fig. 8B, D) at 6, 18, 24, 48, and 72 hpi. As shown, we observed no significant differences in either HR development or H_2O_2 accumulation among four treatments at 6–24 hpi. However, when

compared to *ShARPC3*-overexpression plants (i.e., *arpc3* complementation lines or WT Col-0 overexpression), cell death elicitation was significantly reduced in control and *arpc3* plants at 48 hpi. Moreover, we observed that HR production in *arpc3* plants was much less than that in the control plants at 72 hpi ($P < 0.05$). Consistent with this observation, H_2O_2 production rate was significantly lower in *arpc3* plants than that of other treatments at 48 hpi ($P < 0.05$). Indeed, H_2O_2 accumulation was frequently observed at levels significantly higher in mesophyll cells of *arpc3* plants carrying pCAMBIA3301-*ShARPC3* and WT Col-0 plants carrying pCAMBIA3301-*ShARPC3* than in control plants and *arpc3* mutant plants at 72 hpi. In addition to altered H_2O_2 accumulation and cell death, qRT-PCR analyses revealed that accumulation of *AtARPC3* mRNA was rapidly induced and increased significantly over time in *ShARPC3*-overexpression plants compared to *AtARPC3* mRNA levels in WT Col-0 plants (Supplementary Fig. S4). Conversely, the expression of *AtARPC3* was significantly lower in *arpc3* plants than that in WT Col-0 plants at 0-72 hpi. Taken together, we posit that an increase in *ShARPC3* mRNA accumulation is required for robust defense signaling in response to *On-Lz* infection.

Heterologous expression of ShARPC3 partially rescues the arc18 mutant in Saccharomyces cerevisiae

Saccharomyces cerevisiae growth is sensitive to high temperatures, with optimum growth at 30 °C. To further explore the function of *ShARPC3* in response to temperature stress, *ShARPC3* was expressed in the *S. cerevisiae arc18* mutant strain and transformants were grown under different temperature conditions (e.g., 24 °C, 30 °C, 36 °C, and 42 °C). As shown in Supplementary Fig. S5, the growth *S. cerevisiae* strain Y06714 harboring pDR195-*ShARPC3* was more robust than that of the *arpc3 S. cerevisiae* mutant carrying the empty expression vector pDR195 but was weaker than that of the WT yeast strain, BY4741. Taken together, these data demonstrate that heterologous expression of *ShARPC3* in yeast partially restores the growth at elevated temperatures, suggestive of a functional conservation between *ShARPC3* and yeast *ARC18* and a role in abiotic stress signaling and tolerance.

Discussion

Previous work demonstrated that the Arp2/3 complex is required for actin polymerization and the formation of branched actin networks (Welch *et al.*, 1997). In the current study, and as a function of plant defense signaling, our data reveal a new role for *ShARPC3* during tomato infection by the powdery mildew pathogen *On-Lz*. This is significant, as the current study provides insight into the network of processes that are activated upon pathogen perception and immune signaling. Indeed, we observed that accumulation of *ShARPC3* was rapidly induced during an incompatible interaction, suggesting that *ShARPC3* accumulation might be an early defense activation signal which associated with the stimulation of a large number of primary haustoria. Conversely, and in support of this hypothesis, in the compatible interaction, the expression of *ShARPC3* was down-regulated at all time points – with the exception of 96 hpi – as compared to 0 hpi. In total, these data support the hypothesis that *ShARPC3* is a key regulator of the disease resistance response in tomato against *O. neolyopersici*.

Using a VIGS-based approach, further support for this was revealed by silencing of *ShARPC3* in LA1777, followed by infection with *On-Lz*, led to the development of susceptibility, indicating that *ShARPC3* is a key component of the Arp2/3 complex mediated disease resistance response in tomato against *O. neolyopersici*. While it remains to be investigated, we suggest that this process is likely associated with actin polymerization catalyzed by the Arp2/3 complex, and moreover, functions as a pivotal component in the plant defense signaling cascade (Welch & Mullins, 2002; Tian *et al.*, 2009; Zhang *et al.*, 2017).

In the current study, we provide evidence for a role for *ShARPC3* as a resistance-associated gene activated in response to *On-Lz* infection. We observed that *arpc3* mutant complementation with a 35S-expressing *ShARPC3* construct restores *On-Lz* resistance; in WT Col-0 plants carrying pCAMBIA3301-*ShARPC3*, we observed enhanced resistance to *On-Lz* compared with *arpc3* plants carrying pCAMBIA3301-*ShARPC3* (Fig. 7B). Based on this, it seems plausible that in the case of complementation of *arpc3* by *ShARPC3*, there is also a quantitative effect due to differing levels of *ShARPC3* expression in individual transformants, leading to the observation that *ShARPC3* only partially restores resistance. In

this study, compared to non-silenced resistant LA1777 plants which show a rapid induction of the HR and H₂O₂ accumulation, *ShARPC3*-silenced plants showed a markedly slower HR and H₂O₂ accumulation, responses that coincide with a loss of *On-Lz* resistance. These observations support our previous findings that transcriptomic differences between compatible and incompatible interactions of tomato and *O. neolyopersici* are mainly in timing (Li *et al.*, 2006; Pei *et al.*, 2011). Furthermore, it also indicates that the expression level of *ShARPC3* correlates with the level of *On-Lz* induced HR and H₂O₂ accumulation in tomato, implying that the Arp2/3 complex plays a role in the tomato-*O. neolyopersici* interaction through adjusting the level, and amplitude, of the HR and H₂O₂ accumulation.

As a possible, yet undefined, mechanism underpinning this response, numerous reports have observed that changes in cytoskeletal organization lead to reactive oxygen bursts and subsequent cell death (Gourlay & Ayscough, 2005; Fu *et al.*, 2014; Shimono *et al.*, 2016b; Zhang *et al.*, 2017). Indeed, rearrangement of the plant actin cytoskeleton has been correlated with the activation of defense signaling; most notably, the generation of ROS, changes in gene expression and formation of papillae at the site of penetration (Huot *et al.*, 1998; Gourlay & Ayscough, 2005; Wang *et al.*, 2009). Taken together with our observation of the impact of *ShARPC3* overexpression in Arabidopsis, we posit a role for *ShARPC3* as a positive regulator of immunity in response to *On-Lz* infection.

Our data describe a role for *ShARPC3* associated with SA signaling (Lan *et al.*, 2013; Li & Zou, 2017). Indeed, we observed that SA level was elevated in WT plants following inoculation and was reduced in *ShARPC3*-silenced plants. And tomato can receive the stimuli from *On-Lz* quickly and trigger SA-inducible PR proteins (PR1, PR2, PR3) to protect themselves from being invaded, because the strength of *PR* gene expression has been linked to penetration resistance (Peterhänsel *et al.*, 1997; Van Verk *et al.*, 2008; Molitor *et al.*, 2011). Based on these observations, it is reasonable to assume that SA is involved in the development of resistance to *On-Lz* in tomato, and that modulation of this defense hormone induces the expression of several defense-related genes (e.g., β -1,3-glucanase and chitinase) as observed in other host-pathogen systems (e.g., Mouekouba *et al.*, 2014; Sun *et al.*, 2017). In agreement with our findings, Sun *et al.* (2017) reported that *Glucanase-A*, *Glucanase-B*, *Chitinase-3*, *Chitinase-9* and *PR-1* transcripts significantly changed in the

ϵ -poly-L-lysine-treated + *Botrytis cinerea* infected tomato plants. Interestingly, no significant fitness costs in terms of reduced growth were observed *via* *ShARPC3* silencing, thus making this gene a promising target for mutagenesis to obtain suitable *ShARPC3* alleles for disease resistance breeding in tomato. However, the growth ability of Arabidopsis *arpc3* mutant was weaker than that in WT Col-0 plants. We speculate that the decrease of disease resistance in *arpc3* mutant is due to blocked SA signaling pathways rather than changes in plant size. Rops, as upstream regulators of ARP2/3 complex, can affect the polymerization of microfilament skeleton (Jaffe & Hall, 2005). Poraty-Gavra *et al.*, (2013) indicated that the morphological aberration of Arabidopsis *rop6* mutant results from perturbations that are independent from the SA-associated response. These perturbations uncouple SA-dependent defense signaling from disease resistance execution. Based on the sum of the data presented herein, we hypothesize that *ShARPC3* may function in a similar manner, and moreover, the current study points to a role for the Arp2/3 signaling platform in the control of multiple intercellular signaling processes that are required for immune activation and general stress response signaling.

Materials and Methods

Strains and plant growth

Oidium neolycopersici Lanzhou strain (*On-Lz*) was isolated from tomato plants in Gansu province, China, and was kindly provided by the College of Plant Protection, Northwest A&F University, Yangling, China. The isolate was preserved and propagated on tomato (cv. Moneymaker (MM)) in an environmentally-controlled growth chamber at 20 ± 3 °C with $70 \pm 5\%$ humidity and a 16 h photoperiod.

The *Saccharomyces cerevisiae* diploid mutant strain Y06714 (MATa; *ura310*; *leu210*; *his311*; *met1510*; YLR370c::kanMX4) was grown on SC-U medium at 30 °C, and the WT strain BY4741 (MATa; *his311*; *leu210*; *met1510*; *ura310*) was grown on yeast peptone dextrose (YPD) medium at 30 °C. Yeast strains were obtained from the EUROSCARF collection.

Escherichia coli strain DH5 α was grown on Luria–Bertani (LB) medium containing antibiotics, at 37 °C. *Agrobacterium tumefaciens* strain GV3101 harboring binary vector constructs was grown on antibiotic-containing LB media at 28 °C.

Two tomato genotypes were used in this study: *Solanum lycopersicum* MM and *S. habrochaites* cv. LA1777. LA1777 and *On-Lz* constitute an incompatible interaction, while MM is highly susceptible to *On-Lz*. Tomato seeds were surface sterilized with 3% sodium hypochlorite for 3 min and immediately rinsed with sterile distilled water three times, as previously described (Sun *et al.*, 2018). Seeds were germinated in vermiculite and grown in a growth chamber for seven days under the following environmental conditions: 25 \pm 0.5 °C, 95–100% relative humidity (RH), and continuous illumination of 3500 lux provided by fluorescent lamps. Once the cotyledon leaves had unfolded, the plants were transplanted to soil in 15 cm pots and grown in a temperature-controlled glasshouse (25 \pm 3 °C) for one month before they were used for pathogen inoculation experiments.

Nicotiana benthamiana plants were grown in a growth chamber at 20 °C under a 16-h light/8-h dark cycle with 60% relative humidity and a light intensity of 120-mmol photons m⁻² sec⁻¹.

Arabidopsis thaliana seeds included ecotype Columbia-0 (WT Col-0) and the T-DNA insertion mutant *arpc3* (SALK_099449), were obtained from the Arabidopsis Biological Resource Center (ABRC; The Ohio State University). Seeds were sterilized in 50% bleach (v/v) containing 0.05% Triton X-100 (v/v) for 10 min, rinsed 5 times with sterile water, and incubated at 4 °C for 3 days. For germination, 10 seeds were transferred to 1 mL ½-strength Murashige-Skoog (MS) liquid medium (MS salt supplemented with 0.5% sucrose (w/v), pH 5.5 [pH adjusted to 5.7 by KOH, pH 5.5 after autoclaving], in each well of a 6-well plate) (Wu *et al.*, 2014). Germination and growth took place in a growth chamber at 21 °C and 19 °C during the 8 h day and 16 h night periods, respectively. Relative humidity was 70% and light intensity was 100 W/m².

Sequencing and phylogenetic analysis of ShARPC3

Tomato ARPC3 (Accession number Solyc07g007630) amino-acid sequence was used as a

query in a TBLASTN program against the SGN Tomato Combined database (<http://solgenomics.net/tools/blast/>), in a BLASTP program against an Arabidopsis protein database (<http://www.arabidopsis.org/Blast/index.jsp>), or GenBank using BLASTN (<http://blast.ncbi.nlm.nih.gov/Blast.cgi>) to identify homologous sequences. Conserved and homologous tomato expressed sequence tag (EST) sequences were extracted and assembled. The cDNA sequence of *ShARPC3* was analyzed *in silico* using BLAST and the open reading frame (ORF) Finder software in NCBI (<http://www.ncbi.nlm.nih.gov/gorf/gorf.html>). Multiple sequence alignments were performed using CLUSTALX2.0 (DNASTAR; <http://www.dnastar.com/>) and DNAMAN6.0 (Lynnon BioSoft). Phylogenetic analysis was performed using the MEGA software package (v.6.0; <http://www.megasoftware.net/>) using the neighbor-joining method. The protein domain predictions were assigned based on analysis using the SMART database (<http://smart.embl-heidelberg.de>) and RCSB PDB protein databank (<https://www.rcsb.org/>).

Predicted protein–protein interactions between tomato ARPC3 and other tomato proteins was determined using STRING (<http://string-db.org/>) (Franceschini *et al.*, 2013). To reduce the number of hits (i.e., potential false positives), the minimum required interaction score was set to the highest confidence interval (0.900), and the maximum number of interactors was set to not more than 10 interactors. The subcellular localization of *ShARPC3* protein was predicted from the amino acid sequence using Procomp (v.9.0; <http://linux1.softberry.com/berry.phtml>).

Plasmid construction

The coding sequence (cDNAs) of *ShARPC3* was amplified from reverse-transcribed RNA and cloned using gene-specific DNA primers (Supplementary Table S1). For subcellular localization analysis of *ShARPC3*, the full-length cDNA of *ShARPC3* was cloned into the pCaMV35S::*GFP* vector via *Bam*HI digestion and ligation. For transient expression assays in tobacco, the *ShARPC3* ORF was amplified with DNA primers (Supplementary Table S1) designed to introduce a *Sal*I restriction enzyme site. The amplified product was digested and ligated into the *Sal*I site of the binary vector pGR106 using SmartSeamless Cloning kit. The

VIGS vectors were constructed using tobacco rattle virus (TRV1 and TRV2) according to the methods of Dong *et al.* (2007). The target sequence for *ShARPC3* VIGS started from the non-coding 5' region and included 427 nucleotides of the *ShARPC3* ORF. Selected gene fragments of *ShARPC3* were amplified by PCR from tomato cDNA using the primers *Bam*HI with restriction enzyme site (Supplementary Table S1). The resultant PCR products were ligated into the TRV2 vector using the SmartSeamless Cloning Kit, yielding TRV2:*ShARPC3*. DNA constructs were extracted using the plasmid extracting kit from Qiagen (Shanghai, China) and sequenced to confirm the presence of the intended inserts. For the Arabidopsis *arpc3* mutant complementation assays, PCR-amplified cDNAs of *ShARPC3* (Supplementary Table S1) was subcloned with *Bam*HI digestion site and inserted between 35S promoter and NOS terminator sequences of the binary vector pCAMBIA3301-*ShARPC3* using the SmartSeamless Cloning Kit. For yeast *arc18* mutant complementation assays, PDR195-*ShARPC3* expression constructs were created by cloning PCR-amplified *ShARPC3* cDNA into the *Not*I restriction enzyme (Promega, Madison, WI USA) site of the binary vector PDR195 using the SmartSeamless Cloning Kit (Jieyi Biotech, Shanghai, China).

Subcellular localization analysis

Protoplast isolation from tomato leaves was performed as previously described (Yu *et al.*, 2015), with minor modifications. In brief, leaves of ~8-week-old tomato plants were used for subcellular localization analyses. Leaves were dissected into 0.5-1-mm strips using a razor blade and incubated at room temperature (ca. 22 °C) in 1% cellulase R10 (Yakult Pharmaceutical Ind. Co., Ltd., Tokyo, Japan), 0.25% macerozyme R10 (Yakult Pharmaceutical Ind. Co., Ltd.), 0.4 M mannitol, 20 mM KCl, 10 mM CaCl₂, and 20 mM 2-(N-morpholino)ethanesulfonic acid (MES) for 3–4 h, with shaking at 40–50 rpm. Following incubation at room temperature, the protoplast preparation was filtered through a metal sieve and the eluate was centrifuged at 100 × *g* for 5 min. Pelleted protoplasts were suspended in 5 ml of W5 solution (154 mM NaCl, 125 mM CaCl₂, 5 mM KCl, and 2 mM MES/KOH; pH 5.7) and centrifuged for 5 min at 100 × *g*. The protoplasts were transferred to a tube containing 5 ml of the W5 solution. The protoplasts were pelleted again by centrifugation at 100 × *g* for 5 min and resuspended in 5 ml of the W5 solution. Protoplasts were incubated on ice for 30 min

and then resuspended in 5 ml of MMg buffer (400 mM mannitol, 15 mM MgCl₂, and 4 mM MES/KOH; pH 5.7). For co-transformation, 10 µgs of recombinant plasmid pCaMV35S:*ShARPC3-GFP*, or empty vector pCaMV35S:*GFP* was added to 100 µl of the protoplast suspension. An equal volume of 40% (w/v) PEG3350, freshly prepared with 0.1 M CaCl₂ and 0.8 M mannitol solution, was added. Then, the mixture was incubated at room temperature for 30 min. After incubation, the mixture was diluted with 500 µl of the W5 solution. The solution containing the protoplasts was gently mixed and the protoplasts were pelleted by centrifugation at 100 × *g* for 5 min. Protoplasts were washed twice using the W5 solution, gently re-suspended in 1 ml of W5 solution, and incubated in 12-well plates at room temperature for 18–36 h in the dark. GFP fluorescence was detected using an Olympus FV1000 laser confocal microscope equipped with a 488 nm filter. The experiment was repeated three times.

Agrobacterium-mediated transient expression in Nicotiana benthamiana

The *ShARPC3* gene was amplified using combinations of primers for the PVX (pGR106) assay (Lu *et al.*, 2003). Recombinant plasmid pGR106-*ShARPC3* or pGR106-*GFP* prepared from *Escherichia coli* DH5α was transformed into *Agrobacterium tumefaciens* strain GV3101 via electroporation. Transformants were grown at 28 °C with 50 µg/ml of each of rifampicin and kanamycin until cultures reached stationary growth phase. Cultures of *Agrobacterium* transformed with pGR106-*GFP* or pGR106-*ShARPC3* were centrifuged and the resultant bacterial pellets resuspended in infiltration buffer (10 mM MgCl₂, 150 µM acetosyringone, 10 mM MES pH 5.6) to a final OD 600nm of 0.1. After incubation for 2–3 h in the dark, *A. tumefaciens* cells carrying *ShARPC3*, *GFP*, or buffer was infiltrated. After 24 h, the same infiltration site was challenged with *A. tumefaciens* cells carrying the *BAX* gene. *BAX*, a death-promoting member of the Bcl-2 family of proteins, triggered cell death when expressed in plants (Lacomme & Santa, 1999). *A. tumefaciens* strains carrying *GFP* gene alone was infiltrated in parallel as negative control. Symptom development was monitored visually 5 to 7 d after infiltration. This experiment was repeated three times with each assay consisting of three plants each, with three leaves inoculated.

TRV2-mediated silencing of ShARPC3 in tomato

VIGS TRV1 and TRV2-*ShARPC3* were introduced into *A. tumefaciens* strain GV3101 by heat shock. Five ml of an overnight culture was grown at 28°C in the appropriate antibiotic selection medium in a 15 ml glass tube for 24 h, after which time cultures were spun down and cells were resuspended in infiltration medium (10 mM MES, 10 mM MgCl₂, 200 μM acetosyringone), adjusted to an OD 600nm of 1.0, and incubated at room temperature for 3 h. Agroinfiltration was performed as previously described (Liu *et al.*, 2002). The first and second leaves of four-leaf stage LA1777 plants were infiltrated with a 1:1 mixture of TRV1 and TRV2-*ShARPC3* fragment for the clone. The empty vector TRV2 was used as negative control. To monitor silencing efficiency, plants were inoculated in parallel with TRV2 expressing phytoene desaturase (i.e., TRV2:*ShPDS*; accession number NM_001247166). Following virus inoculation, seedlings were transferred to an environmentally-controlled growth chamber (25 °C, 16-h light/8-h dark photoperiod). Photobleaching symptoms in the PDS control plants were observed ~30 days after virus inoculation. The fourth leaves of plants were inoculated with *On-Lz*, and sampled at 6, 18, 24, 48, and 72 hpi and processed for histological observation. Five plants were inoculated per trial and three biological replicates were performed.

Arabidopsis thaliana transgenic complementation analysis

Arabidopsis genomic DNA preparation was performed as previously described (Qian *et al.*, 2001). SALK_099449 T-DNA insertions in the *AtARPC3* gene were confirmed by PCR and sequencing using the following DNA primers: SALK_099449LP (5'-AAGGTAGAGGCTCAAACGCTC-3'), SALK_099449RP (5'-AGAATCGCCACCTTTAGCTTC-3'), and the T-DNA specific primer LBb1.3 (5'-ATTTTGCCGATTTTCGGAAC-3'). The complete ORF of *ShARPC3* was cloned into the binary expression vector pCAMBIA3301 carrying CaMV35S promoter. pCAMBIA3301-*ShARPC3* was transformed into *Agrobacterium tumefaciens* GV3101 and

was introduced into WT Col-0 and *arpc3* by the floral dip method (Clough & Bent, 1998). Transgenic T1 plants were selected with kanamycin (25 µg/ml) on ½-strength MS medium containing 1% Phytoagar. After 2 weeks, kanamycin-resistant seedlings were transplanted to soil. Three-month-old kanamycin-resistant T2 plants from individual T1 lines were pooled (three or four individuals per sample) and assayed for resistance to *On-Lz* as described below. Kanamycin-resistant siblings of these T2 individuals were confirmed as transgenic by PCR using the following DNA primers: (LP-5'-CGGTGTTCTCTCCAAATGAAATGAACTT-3' and RP-5'-AATTGAGACTTTTCAACAAAGGGTAATA-3') specific to the 35S promoter of the transgene expression construct. The leaves of plants were inoculated with *On-Lz*, sampled at 6, 18, 24, 48, and 72 hpi, and processed for histological observation. Five plants were inoculated per trial and three biological replicates were performed.

Quantitative real time-PCR analysis (qRT-PCR)

To evaluate the expression levels of *ShARPC3* in response to *On-Lz* infection, MM, and LA1777 plant leaves were harvested at 0, 12, 18, 24, 36, 48, 72, and 96 hpi, respectively. For TRV2-mediated silencing of *ShARPC3* assay efficiency the relative expression of *PR1B1* (*PR1*), *Glucanase A* (*PR2*), *Glucanase B* (*PR2-like*), *Chitinase 3* (*PR3*), and *Chitinase 9* (*PR3-like*) (SA pathway-specific gene expression markers, Schenk *et al.*, 2000) were assessed by sampling the fourth leaves of *SIARPC3*-silenced tomato plants at 0, 24, 48, and 72 hpi following infection with *On-Lz*. The *GAPDH* gene was used as the internal control for qRT-PCR analysis (Chalupowicz *et al.*, 2010). DNA primers for qRT-PCR are listed in Supplementary Table S2. For Arabidopsis transgenic complementation assays, leaves were inoculated with *On-Lz* and sampled at 0, 24, 48, and 72 hpi and processed for RNA isolation (below). The *UBQ10* gene was used as the control for qRT-PCR reactions. DNA primers used for qRT-PCR analysis are listed in Supplementary Table S3. Total RNA was prepared using the BIOZOL total RNA extraction kit (Gentaur, Belgium) following the manufacturer's instructions. RNA integrity was evaluated by gel electrophoresis, and the RNA concentration was determined using a Qubit 2.0 Fluorometer (Life Technologies, Thermo-Fisher, Waltham, MA, USA). Total RNA (1 µg) was used for first strand cDNA synthesis using the single strand

cDNA synthesis kit (GeneCopoeia, Rockville, MD, USA) with oligo (dT)₁₈ primer (MBI Fermentas/Thermo-Fisher, Waltham, MA, USA).

The IQTM5 Real-Time PCR System (BioRad, Hercules, CA, USA) was employed for quantitative PCR amplification. For real-time PCR reactions, 1 µl total cDNA was added to a 20 µl PCR reaction mixture containing 10 µl of 2X ultra SYBR mixture (CWBI, Beijing, China), 0.4 µl of each primer, 2 µl template, and 7.2 µl of water. qRT-PCR conditions were as follows: denaturing at 95 °C for 10 min, followed by 40 cycles of 15 sec at 95 °C, 30 sec at 55 °C, 30 sec at 72 °C. Each reaction included a non-template control. All analyses were performed in biological triplicate. Relative transcript quantification was calculated by the comparative 2^{-ΔΔCT} method (Livak & Schmittgen, 2001). Statistical analysis was performed using two-tailed analysis of variance (ANOVA) with the SPSS 17.0 program (IBM SPSS Statistics; <https://www.ibm.com/products/spss-statistics>). A value of *P* < 0.05 indicates a significant difference between groups.

Pathogen inoculation, phenotypic, and histological observations

The fresh *On*-Lz conidia were collected from infected plant leaves with sterile water. Four-week plants were used for inoculation by spraying a spore suspension of 5 × 10⁴ conidia/mL on the whole plants for the histological study. The infection phenotypes of tomato and *A. thaliana* leaves were observed at 7 dpi. For VIGS assay, disease index (DI) was evaluated at 7–14 dpi (Sun *et al.*, 2017). Disease severity was scored according to the following: 0 = no diseased leaves; 1 = 0–5% of leaves having lesions; 3 = leaves with infection lesions up to 6–10%; 5 = leaves with infection lesions up to 11%–20%; 7 = leaves with infection lesions up to 21%–40%; and 9 = leaves with infection lesions up to 41%–100%.

Disease index was calculated using the following equation:

Disease index (DI) = [Σ (number of diseased plant leaves at a given disease severity × the disease severity) / (total plant leaves analyzed × 9)] × 100%. An average DI was calculated at three independent times for each infected plant.

To quantify fungal growth, the number of conidiophores per colony was counted at 7 dpi as previously described (Consonni *et al.*, 2006). At least 25 colonies were counted for each genotype in each experiment. Infection assays and disease severity evaluations were repeated three times. To quantify the accumulation of H₂O₂ (H₂O₂ production rate = H₂O₂ numbers per 100 penetration sites) and the induction of HR cell death (HR production rate = HR numbers per 100 penetration sites) during *On*-Lz infection, 3, 3-diaminobenzidine (DAB) and trypan blue staining were performed following the method of Thordal-Christensen *et al.* (1997). All microscopic examinations were performed using a Nikon Eclipse 80i microscope equipped with DIC (Nikon Corporation, Tokyo, Japan). At least 50 penetration sites on each of four-leaf samples were observed at each time point. Standard errors of deviation were calculated using Microsoft Excel. Statistical significance was assessed by a Student's *t*-test ($P < 0.05$) using SPSS software.

Quantification of Phytohormone Content

Tomato leaves from VIGS experiments were used for phytohormone analysis. Leaves were separately collected at 0, 1, 3, 6, 12, and 24 h after inoculation with *On*-Lz according to Gong *et al.* (2017). Three biological replicates were performed. Standard errors of deviation were calculated using Microsoft Excel. Statistical significance was assessed by a Student's *t*-test ($P < 0.05$) using SPSS software.

Yeast mutant complementation assay

The complete ORF of *ShARPC3* was cloned into pDR195 (Addgene, plasmid #36028). The transformed cell ($\Delta arc18 + ShARPC3$) was obtained by transforming the reconstructed vector (pDR195-*ShARPC3*) into the mutant strain Y06714. The transformed cell containing the empty vector pDR195 ($\Delta arc18 + empty$) was used as a control. To investigate yeast cell survival under stress, transformed cells (initial optical density (OD) of 0.6-1.0 at 600 nm) were cultured in yeast medium. The concentration of pDR195 ($\Delta arc18 + empty$) and

pDR195-*ShARPC3* ($\Delta arc18 + ShARPC3$) transformed cells, as well as WT yeast cells (BY4741) were serially-diluted to 10^7 , 10^6 , 10^5 , 10^4 , and 10^3 (cells/ml) using an Olympus BX-51 microscope (Olympus) coupled with a blood counting chamber. This experiment was repeated three times.

Acknowledgements

The research presented herein was supported by the National Natural Science Foundation of China (grant no. 31571960), Key Industrial Chain Projects of Shaanxi in 2019, Northwest A&F University extension Project (2018–10), and the 111 Project from the Ministry of Education of China (grant no. B07049). Research in the laboratory of B.D. is supported by the U.S. National Science Foundation (IOS-1557437) and the National Institutes of General Medical Sciences (1R01GM125743).

References

- Bai, Y., Huang, C. C., Van Der Hulst, R., Meijer-Dekens, F., & Bonnema, G. (2003). Lindhout P. QTLs for tomato powdery mildew resistance (*Oidium lycopersici*) in *Lycopersicon parviflorum* G1.1601 co-localize with two qualitative powdery mildew resistance genes. *Molecular Plant-Microbe Interactions*, 16, 169-176.
- Bai, Y., Van Der Hulst, R., Bonnema, G., Marcel, T. C., Meijer-Dekens, F., Niks, R., & Lindhout, P. (2005). Tomato defense to *Oidium neolycopersici*: Dominant *OI* genes confer isolate-dependent resistance via a different mechanism than recessive *ol-2*. *Molecular Plant-Microbe Interactions*, 18, 354-362.
- Breitenbach, M., Laun, P., & Gimona, M. (2006). The actin cytoskeleton, RAS-cAMP signaling and mitochondrial ROS in yeast apoptosis. *Trends in Cell Biology*, 15, 637-639.
- Campellone, K. G., & Welch, M. D. (2010). A nucleator arms race: cellular control of actin assembly. *Nature Reviews Molecular Cell Biology*, 11, 237–251.

Caplan, J. L., Mamillapalli, P., Burch-Smith, T. M., Czymmek, K., & Dinesh-Kumar, S. P. (2008). Chloroplastic protein NRIP1 mediates innate immune receptor recognition of a viral effector. *Cell*, 132, 449-462.

Chalupowicz, L., Cohen-Kandli, M., Dror, O., Eichenlaub, R., Gartemann, K. H., Sessa, G., Barash, I., & Manulis-Sasson, S. (2010). Sequential expression of bacterial virulence and plant defense genes during infection of tomato with *Clavibacter michiganensis* subsp. *michiganensis*. *Phytopathology*, 100, 252-261.

Chesarone, M. A., & Goode, B. L. (2009). Actin nucleation and elongation factors: mechanisms and interplay. *Current Opinion in Cell Biology*, 21, 28-37.

Chisholm, S., Coaker, G., Day, B., & Staskawicz, B. J. (2006). Host-microbe interactions: shaping the evolution of the plant immune response. *Cell*, 124, 1-12.

Ciccarese, F., Amenduni, M., Ambrico, A., & Cirulli, M. (2000). The resistance to *Oidium lycopersici* conferred by *ol-2* gene in tomato. *Acta Physiologiae Plantarum*, 22, 266.

Clough, S. J., & Bent, A. F. (1998). Floral dip: a simplified method for *Agrobacterium*-mediated transformation of *Arabidopsis thaliana*. *The Plant Journal*, 16, 735-743.

Consonni, C., Humphry, M. E., Hartmann, H. A., Livaja, M., Durner, J., Westphal, L., Vogel, J., Lipka, V., Kemmerling, B., Schulze-Lefert, P., Somerville, S. C., & Panstruga, R. (2006). Conserved requirement for a plant host cell protein in powdery mildew pathogenesis. *Nature Genetics*, 38, 716-720.

Day, B., Henty, J., Porter, K., & Staiger, C. (2011). The pathogen-actin connection: A platform for defense signaling in plants. *Annual Review of Phytopathology*, 49, 483-506.

- Dong, Y. Y., Burch-Smith, T. M., Liu, Y. L., Mamillapalli, P., & Dinesh-Kumar, S. P. (2007). A ligation-independent cloning tobacco rattle virus vector for high-throughput virus-induced gene silencing identifies roles for NBMADS4-1 and -2 in floral development. *Plant Physiology*, *145*, 1161-1170.
- Feng, H., Wang, X. J., Zhang, Q., Fu, Y. P., Feng, C. X., Wang, B., Huang, L. L., & Kang, Z. S. (2014). Monodehydroascorbate reductase gene, regulated by the wheat PN-2013 miRNA, contributes to adult wheat plant resistance to stripe rust through ROS metabolism. *Biochimica et Biophysica Acta-Gene Regulatory Mechanisms*, *1839*, 1-12.
- Finka, A., Saidi, Y., Goloubinoff, P., Neuhaus, J. M., Zryd, J. P., & Schaefer, D. G. (2008). The knock-out of *ARP3a* gene affects F-actin cytoskeleton organization altering cellular tip growth, morphology and development in moss *Physcomitrella patens*. *Cell Motility and the Cytoskeleton*, *65*, 769-784.
- Franceschini, A., Simonovic, M., Roth, A., Von Mering, C., Szklarczyk, D., Pletscher-Frankild, S., Jensen, L. J., Kuhn, M. M., Lin, J., Minguez, P., & Bork, P. (2013). STRING v9. 1: protein-protein interaction networks, with increased coverage and integration. *Nucleic Acids Research*, *41*, D808-D815.
- Fu, Y., Duan, X., Tang, C., Li, X., Voegelé, R. T., Wang, X., Wei, G., & Kang, Z. (2014). *TaADF7*, an actin-depolymerizing factor, contributes to wheat resistance against *Puccinia striiformis* f. sp. *tritici*. *The Plant Journal*, *78*, 16-30.
- Gong, C., Liu, Y., Liu, S. Y., Cheng, M. Z., Zhang, Y., Wang, R. H., Chen, H. Y., Li, J. F., Chen, X. L., & Wang, A. X. (2017). Analysis of *Clonostachys rosea*-induced resistance to grey mould disease and identification of the key proteins induced in tomato fruit. *Postharvest Biology and Technology*, *123*, 83-93.

Gourlay, C. W., & Ayscough, K. R. (2005). The actin cytoskeleton: a key regulator of apoptosis and ageing. *Nature Reviews Molecular Cell Biology*, 6, 583-589.

Henty-Ridilla, J. L., Shimono, M., Li, J., Chang, J., Day, B., & Staiger, C. J. (2013). The plant actin cytoskeleton responds to signals from microbe-associated molecular patterns. *PLoS Pathogens*, 9, e1003290.

Huibers, R. P., Loonen, A. E. H. M., Gao, D., Ackerveken, G. V. D., Visser, R. G. F., & Bai, Y. (2013). Powdery mildew resistance in tomato by impairment of *SIPMR4* and *SIDMR1*. *PLoS One*, 8, e67467.

Huot, J., Houle, F., Rousseau, S., Deschesnes, R. G., Shah, G. M., & Landry, J. (1998). SAPK2/p38-dependent F-actin reorganization regulates early membrane blebbing during stress-induced apoptosis. *Journal of Cell Biology*, 143, 1361-1373.

Jaffe, A. B., & Hall, A. (2005). Rho GTPases: biochemistry and biology. *Annual Review of Cell and Developmental Biology*, 21, 247-269.

Jones, H., Whipps, J. M., & Guu, S. J. (2001). The tomato powdery mildew fungus *Oidium neolycopersici*. *Molecular Plant Pathology*, 2, 303-309.

Jones, J. D., & Dangl, J. L. (2006). The plant immune system. *Nature*, 444, 323-329.

Kim, H., Park, M., Kim, S. J., & Hwang, I. (2005). Actin filaments play a critical role in vacuolar trafficking at the Golgi complex in plant cells. *Plant Cell*, 17, 888-902.

Kobayashi, I., Kobayashi, Y., & Hardham, A. R. (1994). Dynamic reorganization of microtubules and microfilaments in flax cells during the resistance response to flax rust infection. *Planta*, 195, 237-247.

Kotchoni, S. O., Zakharova, T., Mallery, E. L., Le, J., El-Assal, S. E., & Szymanski, D. B.

- (2009). The association of the Arabidopsis actin-related protein2/3 complex with cell membranes is linked to its assembly status but not its activation. *Plant Physiology*, 151, 2095-2109.
- Lacomme, C., & Santa, C. S. (1999). Bax-induced cell death in tobacco is similar to the hypersensitive response. *Proceedings of the National Academy of Sciences*, 96, 7956-7961.
- Lan, A., Huang, J., Zhao, W., Peng, Y., Chen, Z., & Kang, D. (2013). A salicylic acid-induced rice (*Oryza sativa* L.) transcription factor OsWRKY77 is involved in disease resistance of *Arabidopsis thaliana*. *Plant Biology*, 15, 452-461.
- Lebeda, A., Mieslerová, B., Petřivalský, M., Luhová, L., Špundová, M., Sedlářová, M., Nožková-Hlaváčková, V., Pink, D. A. C. (2014). Resistance mechanisms of wild tomato germplasm to infection of *Oidium neolycopersici*. *European Journal of Plant Pathology*, 138 (S1), 569-596.
- Li, C. W., Bai, Y. L., Jacobsen, E., Visser, R., Lindhout, P., & Bonnema, G. (2006). Tomato defense to the powdery mildew fungus: differences in expression of genes in susceptible, monogenic- and polygenic resistance responses are mainly in timing. *Plant Molecular Biology*, 62, 127-140.
- Li, L., & Zou, Y. (2017). Induction of disease resistance by salicylic acid and calcium ion against *Botrytis cinerea* in tomato (*Lycopersicon esculentum*). *Emirates Journal of Food Agriculture*, 29, 78-82.
- Li, P., & Day, B. (2019). Battlefield Cytoskeleton: Cytoskeletal regulation and pathogen targeting of plant immunity. *Mol Plant-Microbe Interact*. doi: 10.1094/MPMI-07-18-0195-FI.

Lindhout, P., Pet, G., & van der Beek, H. (1994a). Screening wild *Lycopersicon* species for resistance to powdery mildew (*Oidium lycopersicum*). *Euphytica*, 72, 43-49.

Lindhout, P., van der Beek, H., & Pet, G. (1994b). Wild *Lycopersicon* species as sources for resistance to powdery mildew (*Oidium lycopersicum*): Mapping of resistance gene *OI-1* on chromosome 6 of *Lycopersicon hirsutum*. *Acta Horticulturae*, 376, 387-394.

Liu, Y. L., Schiff, M., Marathe, R., & Dinesh-Kumar, S. P. (2002). Tobacco *Rar1*, *EDS1* and *NPR1/NIM1* like genes are required for N-mediated resistance to tobacco mosaic virus. *The Plant Journal*, 30, 415-429.

Livak, K. J., & Schmittgen, T. D. (2001). Analysis of relative gene expression data using real-time quantitative PCR and the $2^{-\Delta\Delta CT}$ method. *Methods*, 25, 402-408.

Lu, R., Malcuit, I., Moffett, P., Ruiz, M. T., Peart, J., Wu, A. J., Rathjen, J. P., Bendahmane, A., Day, L., & Baulcombe, D. C. (2003). High throughput virus-induced gene silencing implicates heat shock protein 90 in plant disease resistance. *EMBO Journal*, 22, 5690-5699.

Machesky, L. M., & Gould, K. L. (1999). The Arp2/3 complex: a multifunctional actin organizer. *Current Opinion in Cell Biology*, 11, 117-121.

Machesky, L. M., Atkinson, S. J., Ampe, C., Vandekerckhove, J., & Pollard, T. D. (1994). Purification of a cortical complex containing two unconventional actins from *Acanthamoeba* by affinity chromatography on profilin-agarose. *Journal of Cell Biology*, 127, 107-116.

Machesky, L. M., Mullins, R. D., Higgs, H. N., Kaiser, D. A., Blanchoin, L., May, R. C., Hall, M. E., & Pollard, T. D. (1999). Scar, a WASP-related protein, activates nucleation of actin filaments by the Arp2/3 complex. *Proceedings of the National Academy of Science of the*

United States of America, 96, 3739-3744.

Maisch, J., Fiserova, J., Fischer, L., & Nick, P. (2009). Tobacco Arp3 is localized to actin-nucleating sites *in vivo*. *Journal of Experimental Botany*, 60, 603-614.

Marcel, T. C., Gorguet, B., Ta, M. T., Kohutova, Z., Vels, A., & Niks, R. E. (2008). Isolate specificity of quantitative trait loci for partial resistance of barley to *Puccinia hordei* confirmed in mapping populations and near-isogenic lines. *New Phytologist*, 177, 743-755.

Mathur, J., Mathur, N., Kernebeck, B., & Hülkamp, M. (2003a). Mutations in actin-related proteins 2 and 3 affect cell shape development in *Arabidopsis*. *The Plant Cell*, 15, 1632-1645.

Mathur, J., Mathur, N., Kirik, V., Kernebeck, B., Srinivas, B. P., & Hülkamp, M. (2003b). *Arabidopsis*, *CROOKED* encodes for the smallest subunit of the ARP2/3 complex and controls cell shape by region specific fine F-actin formation. *Development*, 130, 3137-3146.

Mathur, J., & Hülkamp, M. (2002). Microtubules and microfilaments in cell morphogenesis in higher plants. *Current Biology*, 12, R669-R676.

Mieslerová, B., Lebeda, A., & Kennedy, R. (2004). Variation in *Oidium neolycopersici* development on host and non-host plant species and their tissue defence response. *Annals of Applied Biology*, 144, 237-248.

Molitor, A., Zajic, D., Voll, L. M., Pons, K. H. J., Samans, B., Kogel, K. H., & Waller, F. (2011). Barley leaf transcriptome and metabolite analysis reveals new aspects of compatibility and *Piriformospora indica*-mediated systemic induced resistance to powdery mildew. *Molecular Plant-Microbe Interactions*, 24, 1427-1439.

Mouekouba, L. D., Zhang, L., Guan, X., Chen, X., Chen, H., Zhang, J., Zhang, J., Li, J., Yang, Y., & Wang, A. (2014). Analysis of *Clonostachys rosea*-induced resistance to tomato gray mold disease in tomato leaves. *PLoS One*, 9, e102690.

Mur, L. A. J., Kenton, P., Lloyd, A. J., Ougham, H., & Prats, E. (2008). The hypersensitive response; the centenary is upon us but how much do we know? *Journal of Experimental Botany*, 59, 501-520.

Nakajima, M., & Akutsu, K. (2014). Virulence factors of *Botrytis cinerea*. *Journal of General Plant Pathology*, 80, 15-23.

Nelson, R., Wiesner-Hanks, T., Wisser, R., & Balint-Kurti, P. (2018). Navigating complexity to breed disease resistant crops. *Nature Reviews Genetics*, 19, 21-33.

Opalski, K. S., Schultheiss, H., Kogel, K. H., & Hüchelhoven, R. (2005). The receptor-like MLO protein and the RAC/ROP family G-protein RACB modulate actin reorganization in barley attacked by the biotrophic powdery mildew fungus *Blumeria graminis* f.sp. *hordei*. *The Plant Journal*, 41, 291-303.

Pantaloni, D., le Clainche, C., & Carlier, M. F. (2001). Mechanism of actin-based motility. *Science*, 292, 1502-1506.

Pei, D. L., Ma, H. Z., Zhang, Y., Ma, Y. S., Wang, W. J., Geng, H. X., Wu, J. Y., & Li, C. W. (2011). Silencing a putative cytosolic NADP-malic enzyme gene compromised tomato resistance to *Oidium neolycopersici*. *Life Science Journal*, 8, 652-657.

Peterhänsel, C., Freialdenhoven, A., Kurth, J., Kolsch, R., & Schulze-Lefert, P. (1997). Interaction analyses of genes required for resistance responses to powdery mildew in barley reveal distinct pathways leading to leaf cell death. *The Plant Cell*, 9, 1397-1409.

Pollard, T. D., & Borisy, G. G. (2003). Cellular motility driven by assembly and disassembly of actin filaments. *Cell*, 112, 453-465.

Pollard, T. D., Blanchoin, L., & Mullins, R. D. (2000). Molecular mechanisms controlling actin filament dynamics in nonmuscle cells. *Annual Review of Biophysics and Biomolecular Structure*, 29, 545-576.

Poraty-Gavra, L., Zimmermann, P., Haigis, S., Bednarek, P., Hazak, O., Stelmakh, O. R., Sadot, E., Schulze-Lefert, P., Gruissem, W., & Yalovsky, S. (2013). The Arabidopsis Rho of plants GTPase AtROP6 functions in developmental and pathogen response pathways. *Plant Physiology*, 161, 1172-1188.

Porter, K., & Day, B. (2015). From filaments to function: The role of the plant actin cytoskeleton in pathogen perception, signaling, and immunity. *Journal of Integrative Plant Biology*, 58, 299-311.

Qi, T., Wang, J., Sun, Q., Day, B., Guo, J., & Ma, Q. (2017). *TaARPC3*, Contributes to wheat resistance against the stripe rust fungus. *Frontiers in Plant Science*, 8, doi:10.3389/fpls.2017.01245.

Qian, Q., Li, Y. H., Zeng, D., Teng, S., Wang, Z., Li, X., Dong, Z., Dai, N., Sun, L., & Li, J. (2001). Isolation and genetic characterization of a fragile plant mutant rice (*Oryza sativa* L.). *Chinese Science Bulletin*, 46, 2082-2085.

Roberts, P., Momol, T., & Pernezny, K. (2002). Powdery mildew on tomato, document PP-191 of Plant Pathology Department, Florida Cooperative Extension Service, Institute of Food and Agricultural Sciences, University of Florida.

Rohatgi, R., Ma, L., Miki, H., Lopez, M., Kirchhausen, T., Takenawa, T., & Kirschner, M. W.

(1999). The interaction between N-WASP and the Arp2/3 complex links Cdc42-dependent signals to actin assembly. *Cell*, 97, 221-231.

Schenk, P. M., Kazan, K., Wilson, I., Anderson, J. P., Richmond, T., Somerville, S. C., & Manners, J. M. (2000). Coordinated plant defense responses in *Arabidopsis* revealed by microarray analysis. *Proceedings of the National Academy of Sciences*, 97, 11655-11660.

Shimono, M., Higaki, T., Kaku, H., Shibuya, N., Hasezawa, S., & Day, B. (2016a). Quantitative evaluation of stomatal cytoskeletal patterns during the activation of immune signaling in *Arabidopsis thaliana*. *PLoS One*, 11, e0159291.

Shimono, M., Lu, Y., Porter, K., Kvitko, B., Creason, A., Henty-Ridilla, J., He, S. Y., Chang, J. H., Staiger, C., & Day, B. (2016b). The *Pseudomonas syringae* type III effector HopG1 induces actin filament remodeling in *Arabidopsis* in association with disease symptom development. *Plant Physiology*, 171, 2239-2255.

Sparkes, I., Runions, J., Hawes, C., & Griffing, L. (2009). Movement and remodeling of the endoplasmic reticulum in non-dividing cells of tobacco leaves. *The Plant Cell* 21, 3937-3949.

Sun GZ, Wang H, Shi BB, Shangguan NN, Wang Y, Ma Q. 2017. Control efficiency and expressions of resistance genes in tomato plants treated with ϵ -poly-L-lysine against *Botrytis cinerea*. *Pesticide Biochemistry and Physiology*, 143, 191-198.

Sun, G. Z., Yang, Q. C., Zhang, A. C., Guo, J., Liu, X. J., Wang, Y., & Ma, Q. (2018). Synergistic effect of the combined bio-fungicides ϵ -poly-L-lysine and chitooligosaccharide in controlling grey mould (*Botrytis cinerea*) in tomatoes. *International Journal of Food Microbiology*, 276, 46-53.

Takenawa, T., & Miki, H. (2001). WASP and WAVE family proteins: key molecules for rapid

rearrangement of cortical actin filaments and cell movement. *Journal of Cell Science*, 114, 1801-1809.

Takken, F. L., Albrecht, M., & Tameling, W. I. (2006). Resistance proteins: molecular switches of plant defence. *Current Opinion in Plant Biology*, 9, 383-390.

Thordal-Christensen, H., Zhang, Z. G., Wei, Y. D., & Collinge, D. B. (1997). Subcellular localization of H₂O₂ in plants. H₂O₂ accumulation in papillae and hypersensitive response during the barley-powdery mildew interaction. *The Plant Journal*, 11, 1187-1194.

Tian, M., Chaudhry, F., Ruzicka, D. R., Meagher, R. B., Staiger, C. J., & Day, B. (2009). *Arabidopsis* actin-depolymerizing factor *AtADF4* mediates defense signal transduction triggered by the *Pseudomonas syringae* effector *AvrPphB*. *Plant Physiology*, 150, 815-824.

Van Verk, M. C., Pappaioannou, D., Neeleman, L., Bol, J. F., & Linthorst, H. J. (2008). A novel WRKY transcription factor is required for induction of *PR-1a* gene expression by salicylic acid and bacterial elicitors. *Plant Physiology*, 146, 1983-1995.

Wang, X., Tang, C., Zhang, G., Li, Y., Wang, C., Liu, B., Qu, Z. P., Zhao, J., Han, Q. M., Huang, L. L., Chen, X. M., & Kang, Z. S. (2009). cDNA-AFLP analysis reveals differential gene expression in compatible interaction of wheat challenged with *Puccinia striiformis* f. sp. *tritici*. *BMC Genomics*, 10, 289.

Weaver, A. M., Young, M. E., Lee, W. L., & Cooper, J. A. (2003). Integration of signals to the Arp2/3 complex. *Current Opinion in Cell Biology*, 15, 23-30.

Welch, M. D., Holtzman, D. A., & Drubin, D. G. (1994). The yeast actin cytoskeleton. *Current Opinion in Cell Biology*, 6, 110-119.

Welch, M. D., Iwamatsu, A., & Mitchison, T. J. (1997). Actin polymerization is induced by Arp2/3 protein complex at the surface of *Listeria monocytogenes*. *Nature*, 385, 265-268.

Welch, M. D., & Mullins., R. D. (2002). Cellular control of actin nucleation. *Annual Review of Cell Developmental Biology*, 18, 247-288.

Wu, H. Y., Liu, K. H., Wang, Y. C., Wu, J. F., Chiu, W. L., Chen, C. Y., Wu, S. H., Sheen, J., & Lai, E. M. (2014). AGROBEST: an efficient *Agrobacterium*-mediated transient expression method for versatile gene function analyses in *Arabidopsis* seedlings. *Plant Methods*, 10, 19.

Yokota, K., Fukai, E., Madsen, L. H., Jurkiewicz, A., Rueda, P., Radutoiu, S., Held, M., Hossain, M. S., Szczyglowski, K., Morieri, G., Oldroyd, G. E. D., Downie, J. A., Nielsen, M. W., & Rusek, A. M. (2009). Rearrangement of actin cytoskeleton mediates invasion of *Lotus japonicus* roots by *Mesorhizobium loti*. *Plant Cell*, 21, 267-284.

Yu, H., Jiang, W., Liu, Q., Zhang, H., Piao, M. X., Chen, Z. D., & Bian, M. D. (2015). Expression pattern and subcellular localization of the ovate protein family in rice. *PLoS One*, 10, e0118966.

Zhang, B., Yuan, H., Wang, J., Huo, Y., Shimono, M., Day, B., & Ma, Q. (2017). TaADF4, an actin-depolymerizing factor from wheat, is required for resistance to the stripe rust pathogen *Puccinia striiformis* f. sp. *tritici*. *The Plant Journal*, 89, 1210-1224.

Zhang, R., Xia, X., Lindsey, K., & Da, R. P. (2012). Functional complementation of *dwf4* mutants of *Arabidopsis* by overexpression of *CYP724A1*. *Journal of Plant Physiology*, 169, 421-428.

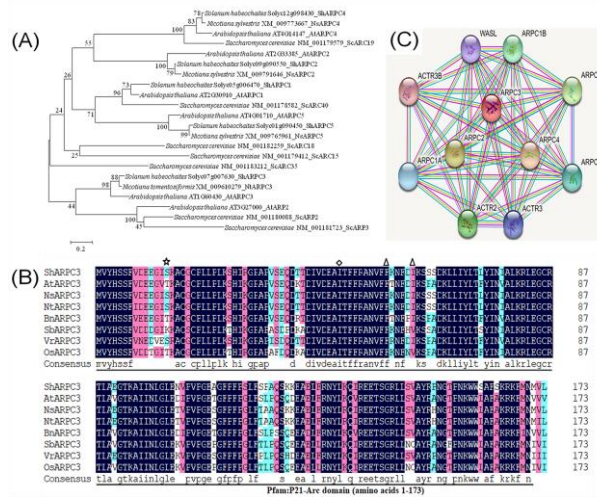


Fig.1. Sequence analysis and predicted interaction network of tomato actin related protein 2 and 3 (Arp2/3) complex subunit 3 (*ShARPC3*). (A) Evolutionary analysis of *ShARPC3*. Analysis was conducted using the neighbor-joining method in MEGA6.0. Representative phylogenetic tree of *ShARPC3* and ARP2/3 complex sequences from *S. habrochaites* (*ShARP2/3*), *A. thaliana* (*AtARP2/3*), *N. sylvestris* (*NsARP2/3*), *N. tomentosiformis* (*NtARP2/3*) and *S. cerevisiae* (*ScARP2/3*). Accession numbers are shown after the gene names. *ShARPC3*, encoded by the tomato gene *Solyc07g007630*, is considered to be the tomato ortholog of *NtARPC3* and *AtARPC3*. (B) Multiple protein sequence alignment of *ShARPC3* and characterized members of ARPC3 proteins. Sequence alignment of *ShARPC3* (*Solyc07g007630*), *AtARPC3* (*AT1G60430*), *NsARPC3* (*XP_009791878*), *NtARPC3* (*XP_009608574*), *BnARPC3* (*XP_022548276*), *SbARPC3* (*XP_002451839*), *VrARPC3* (*XP_014510301*), and *OsARPC3* (*XP_015626361*). The *ShARPC3* sequence encodes a 174-amino-acid protein containing one P21-Arc domain (amino acids 1-173), one glycyl lysine isopeptide (Lys-Gly) (interchain with G-Cter in SUMO2)-cross-link site (amino acid 14) is highlighted with asterisk, one phosphotyrosine-modified residue (amino acid 47) is highlighted with a diamond, two N6-acetyllysine-modified residues (amino acids 56 and 61) are highlighted with a triangle. Amino acid similarity are shown within the Pfam:P21-Arc domain. Black boxes indicate regions of 100% homology, pink boxes indicate $\geq 75\%$ homology, and cyan boxes highlight $\geq 50\%$ homology. (C) The network map showed the interaction of *ShARPC3* with other tomato proteins according to STRING database analysis. Here, the ARPC1A node in the figure represents the unknown 3D structure, whereas other nodes indicate the availability of known or predicted 3D structures. The red colored node

represents the query protein. The edge, colored in turquoise, yellow, purple, and white, indicates that the prediction was made based on curated databases, text-mining, experimentally determined, and/or protein homology, respectively.

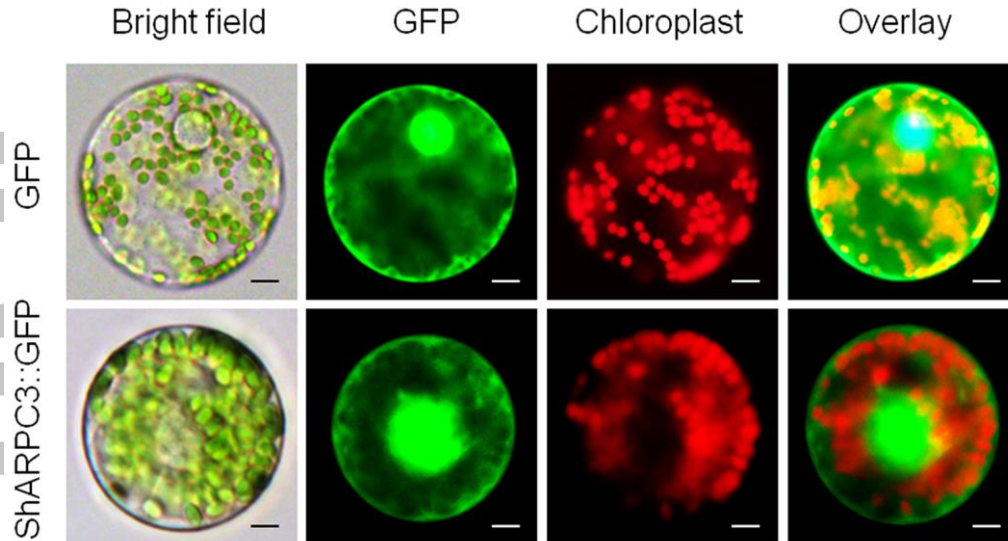


Fig. 2. Subcellular localization of *ShARPC3*. Protoplast transient expression using *GFP-ShARPC3* fusion constructs was used to determine the subcellular localization. The $35S::GFP-ShARPC3$ constructs were transformed into a tomato protoplast cell. Fluorescence images of GFP and chlorophyll autofluorescence (Chl) were captured by laser confocal scanning microscopy, as indicated by green and red emission signals, respectively (scale bars, 20 μ m).

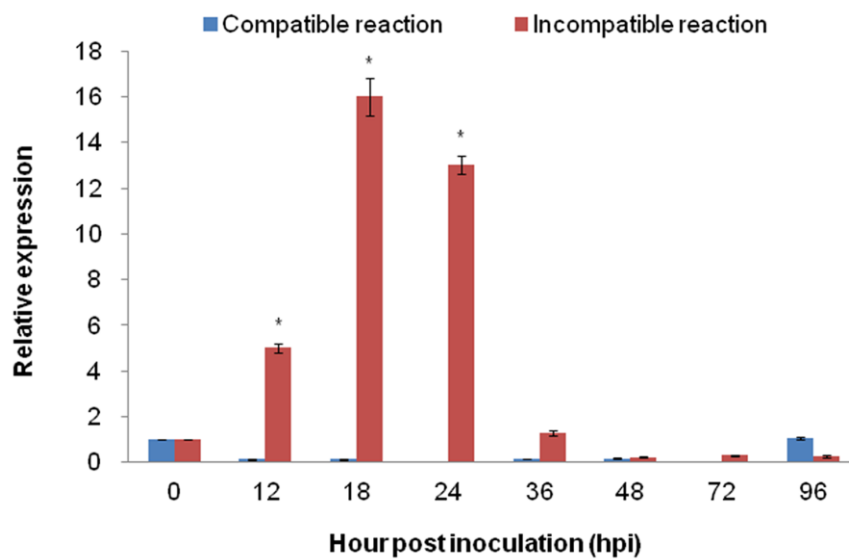


Fig. 3. Quantitative real-time PCR expression analysis of *ARPC3* in tomato leaves. The expression level of *ARPC3* in tomato leaves was induced in incompatible reaction between tomato-*On*-Lz interaction. Error bars represent standard deviation from three independent replicates. Asterisks (*) indicate significant difference ($P < 0.05$) from 0 hpi using Student's *t*-test.

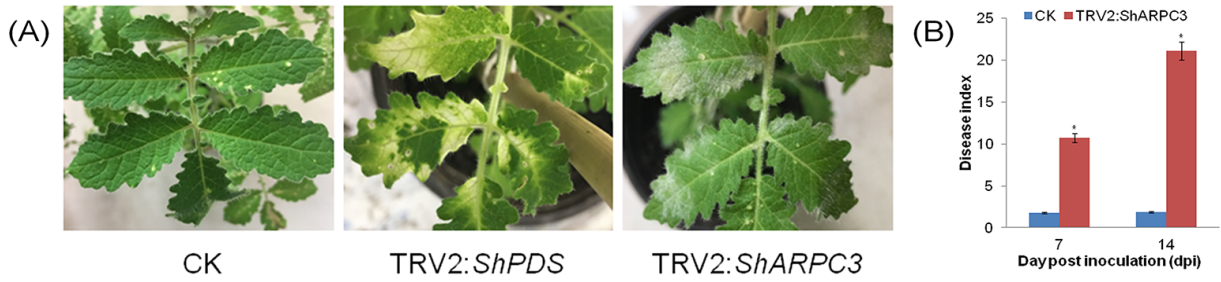


Fig. 4. Silencing of *ShARPC3* in tomato LA1777 renders plants susceptible to *On-Lz*. (A) Infection phenotypes of CK (TRV2), TRV2:*ShPDS*, TRV2:*ShARPC3* tomato leaves at 7 dpi. (B) Disease indexes of CK and TRV2:*ShARPC3* plants at 7 and 14 dpi, respectively. Error bars represent the variations among three independent replicates. The asterisk (*) indicates statistically significant differences in disease index between CK (TRV2) and TRV2:*ShARPC3* plants according to independent-samples *t*-test ($P < 0.05$).

Accepted Article

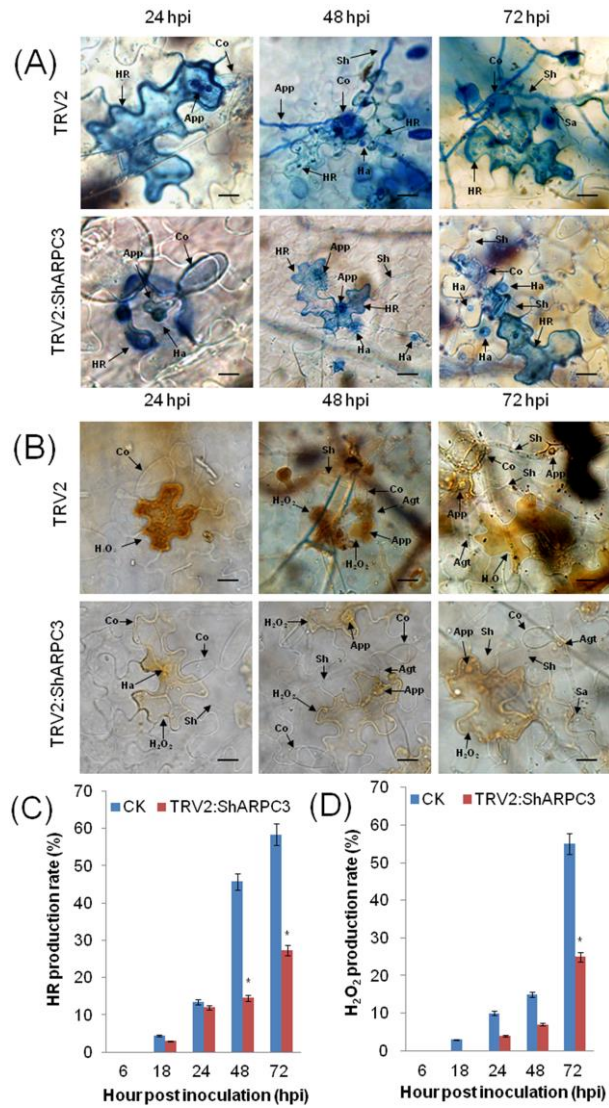


Fig. 5. Silencing of *ShARPC3* in tomato reduced defense responses and increased *On-Lz* infection. (A) Histological observation of hypersensitive cell death in CK (TRV2) and TRV2:*ShARPC3* tomato leaves inoculated with *On-Lz* by microscopy. Blue (trypan) staining indicates hypersensitive cell death. (B) Histological observation of H₂O₂ accumulation in CK and TRV2:*ShARPC3* tomato leaves inoculated with *On-Lz* by microscopy. (C) HR production rate of tomato leaves carrying TRV2 (CK) or TRV2:*ShARPC3* at 6, 18, 24, 48, and 72 hpi, respectively. (D) H₂O₂ production in CK or TRV2:*ShARPC3* tomato leaves at 6, 18, 24, 48, and 72 hpi, respectively. Co, conidium; App, appressorium; Agt, appressorium germ tube; Ha, haustorium; Pa, papilla; Sh, secondary hyphae; Sa, secondary appressorium; HR, hypersensitive response. Bar, 50 μm. Error bars represent the variations among three independent replicates. The asterisk (*) indicates statistically significant differences between CK (TRV2) and TRV2:*ShARPC3* plants ($P < 0.05$).

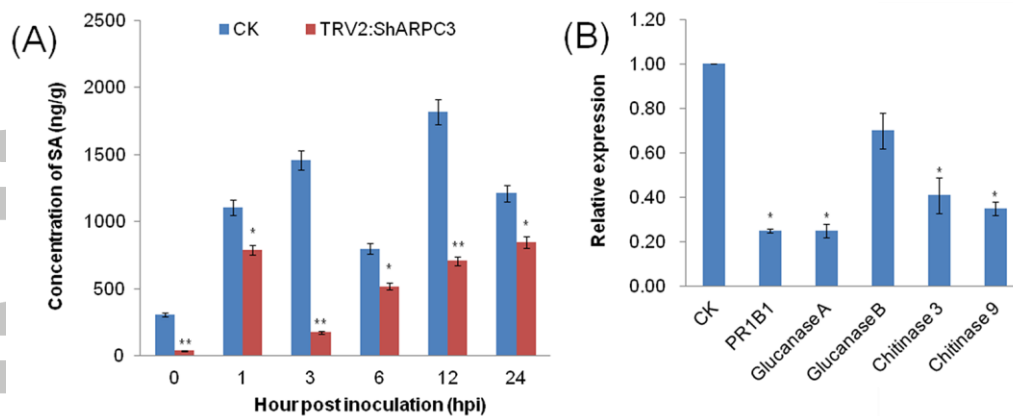


Fig. 6. SA content and relative mRNA transcript levels of *PRs* genes are reduced in *On-Lz*-inoculated *ShARPC3*-silenced plants. (A) Changes in SA levels in tomato leaves carrying TRV2 (CK) or TRV2:*ShARPC3* at 0, 1, 3, 6, 12, and 24 hpi, respectively. (B) Relative mRNA transcript levels of *PR1B1* (*PR1*), β -1,3-glucanase (*PR2*), and *chitinase* (*PR3*) (SA pathway-specific gene expression markers) in CK and TRV2:*ShARPC3* tomato leaves at 24 hpi as determined by quantitative real-time PCR. Error bars represent the variations among three independent replicates. Number of asterisks indicate statistically degree of significance between CK (TRV2) and TRV2:*ShARPC3* plants (Student's t-test, * $P < 0.05$; ** $P < 0.01$).

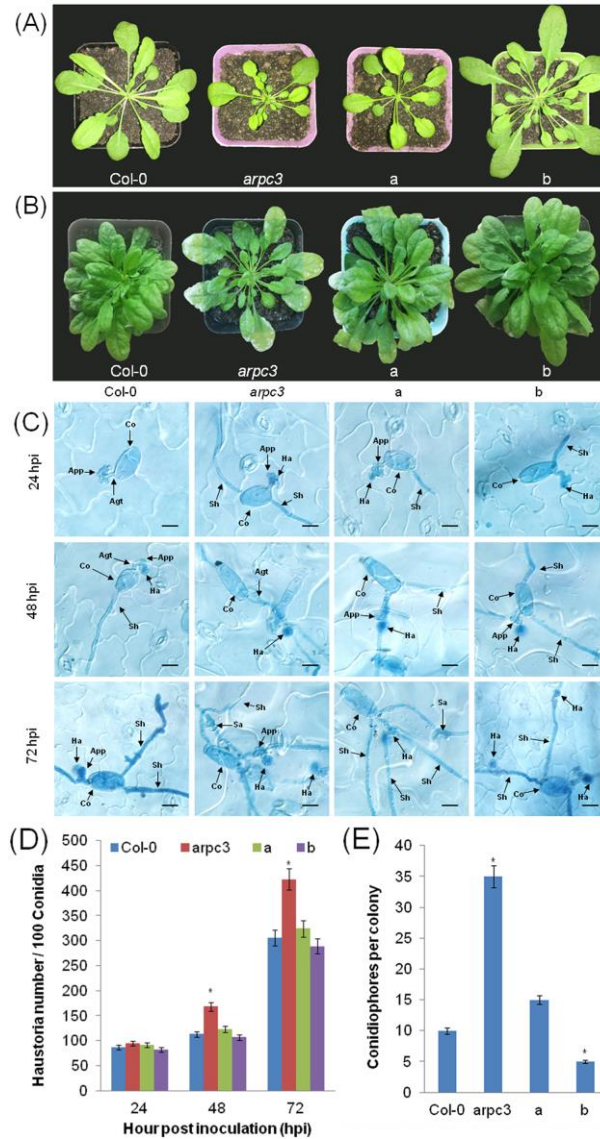


Fig. 7. Complementation of *ShARPC3* function confers *On-Lz* resistance in *A. thaliana*. (A) Macroscopic phenotypes of representative unchallenged plants at 8 weeks. (B) Infection phenotypes of WT Col-0 plants, *arpc3* mutants, *arpc3* plants transgenic plants expressing pCAMBIA3301-*ShARPC3*, and WT Col-0 transgenic plants expressing pCAMBIA3301-*ShARPC3*. Images were taken at 7 dpi. (C) Infection process of conidiation in WT Col-0 plants, *arpc3* mutants, *arpc3* plants transgenic plants expressing pCAMBIA3301-*ShARPC3*, and WT Col-0 transgenic plants expressing pCAMBIA3301-*ShARPC3* by microscopy. Images were taken at 24 hpi, 48 hpi, and 72 hpi. (D) Quantitative assessment of haustoria/100 conidia on WT Col-0 plants, the *arpc3* mutant, the *arpc3* mutant expressing pCAMBIA3301-*ShARPC3*, and WT Col-0 plants expressing pCAMBIA3301-*ShARPC3*. Images were taken at 24 hpi, 48 hpi, and 72 hpi.

(E) Quantitative assessment of conidiation on WT Col-0 plants, the *arpc3* mutant, the *arpc3* mutant expressing pCAMBIA3301-*ShARPC3*, and WT Col-0 plants expressing pCAMBIA3301-*ShARPC3*. Images were taken at 7 dpi. a: *arpc3* plants transgenic expressing pCAMBIA3301-*ShARPC3*; b: WT Col-0 plants expressing pCAMBIA3301-*ShARPC3*. Error bars represent the variations among three independent replicates. Asterisks (*) indicate a significant difference between WT Col-0 plants, *arpc3* mutants, *arpc3* plants expressing pCAMBIA3301-*ShARPC3*, and WT Col-0 plants expressing pCAMBIA3301-*ShARPC3* ($P < 0.05$).

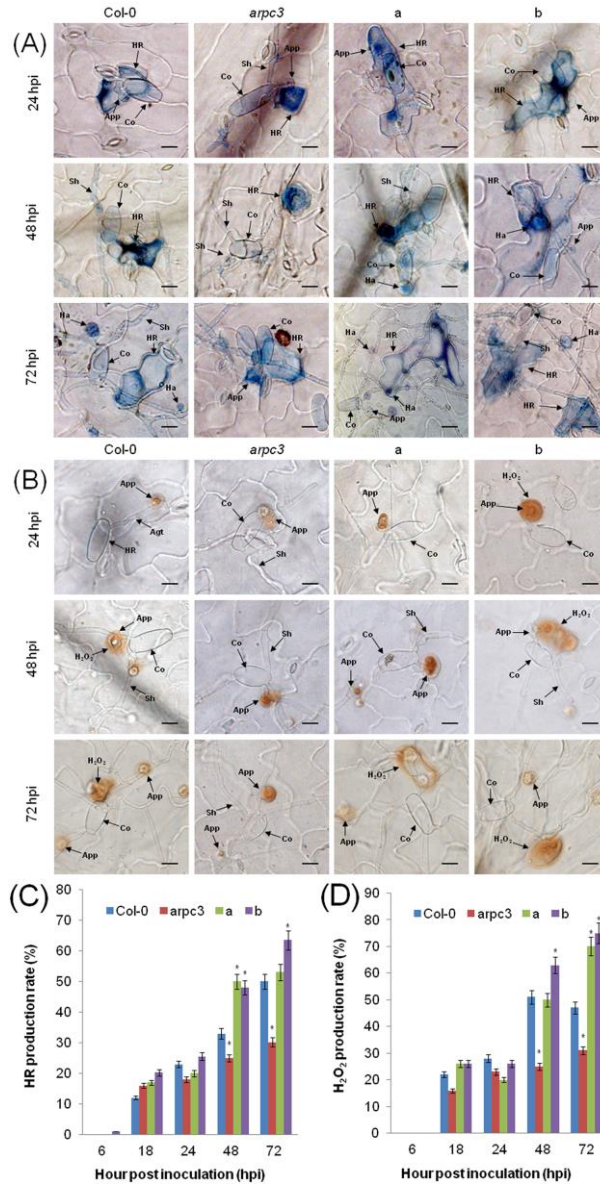


Fig. 8. Overexpression of *ShARPC3* in *A. thaliana* leads to enhanced defense responses. (A) Histological observation of hypersensitive cell death in WT Col-0 plants, the *arpc3* mutant, the *arpc3* mutant expressing pCAMBIA3301-*ShARPC3*, and WT Col-0 plants expressing pCAMBIA3301-*ShARPC3* inoculated with *On-Lz* by microscopy. Blue (trypan) staining indicates hypersensitive cell death. (B) Histological observation of H₂O₂ accumulation in WT Col-0 plants, the *arpc3* mutant, the *arpc3* mutant expressing pCAMBIA3301-*ShARPC3*, and WT Col-0 plants expressing pCAMBIA3301-*ShARPC3* inoculated with *On-Lz* by microscopy. (C) HR production rate in WT Col-0 plants, *arpc3* mutants, *arpc3* transgenic plants expressing pCAMBIA3301-*ShARPC3*, and WT Col-0 plants expressing pCAMBIA3301-*ShARPC3* at 6, 18, 24, 48, and 72 hpi, respectively. (D) H₂O₂ production rate of Col-0 plants, *arpc3* mutants,

arpc3 plants transgenic for pCAMBIA3301-*ShARPC3*, and WT Col-0 plants transgenic for pCAMBIA3301-*ShARPC3* at 6, 18, 24, 48, and 72 hpi, respectively. Co, conidium; App, appressorium; Agt, appressorium germ tube; Ha, haustorium; Pa, papilla; Sh, secondary hyphae; Sa, secondary appressorium; HR, hypersensitive response. Bar, 50 μ m. a: *arpc3* plants transgenic for pCAMBIA3301-*ShARPC3*; b: WT Col-0 plants expressing pCAMBIA3301-*ShARPC3*. Error bars represent the absolute variations in conidia number among three independent biological replicates. Asterisks (*) indicate a significant difference between WT Col-0 plants and *arpc3* mutants and *arpc3* plants transgenic expressing pCAMBIA3301-*ShARPC3*, as well as WT Col-0 plants expressing pCAMBIA3301-*ShARPC3* ($P < 0.05$).

Accepted Article